Supplementary Information for

Molecular Mechanism of Respiratory Syncytial Virus Fusion Inhibitors

Michael B. Battles[1], Johannes P. Langedijk[2], Polina Furmanova-Hollenstein[2], Supranee Chaiwatpongsakorn[3], Heather M. Costello[3], Leen Kwanten[4], Luc Vranckx[4], Paul Vink[5], Steffen Jaensch[5], Tim Jonckers[6], Anil Koul[4], Eric Arnoult[7], Mark E. Peeples[3,8], Dirk Roymans[4] and Jason S. McLellan[1*]

[1]Department of Biochemistry, Geisel School of Medicine at Dartmouth, Hanover, NH, 03755 USA.

[2]Janssen Infectious Diseases and Vaccines, Archimedesweg 4-6, 2333 CN Leiden, Netherlands.

[3]Center for Vaccines & Immunity, The Research Institute at Nationwide Children's Hospital, Columbus, OH, 43205 USA.

[4]Respiratory Infections Research & [6]Medicinal Chemistry Department, Janssen Infectious Diseases & Vaccines BVBA, Turnhoutseweg 30, 2340 Beerse, Belgium.

[5]Discovery Sciences, Janssen Pharmaceutica NV, Turnhoutseweg 30, 2340 Beerse, Belgium.

[7]Computational Chemistry, Janssen R&D LLC, 1400 McKean Road, Spring House, PA, 19477 USA.

[8]Department of Pediatrics, The Ohio State University College of Medicine, Columbus, OH 43205 USA.

*Correspondence to: Jason.S.McLellan@Dartmouth.edu

This document contains:

Nature Chemical Biology: doi:10.1038/nchembio.1982

Supplementary Results

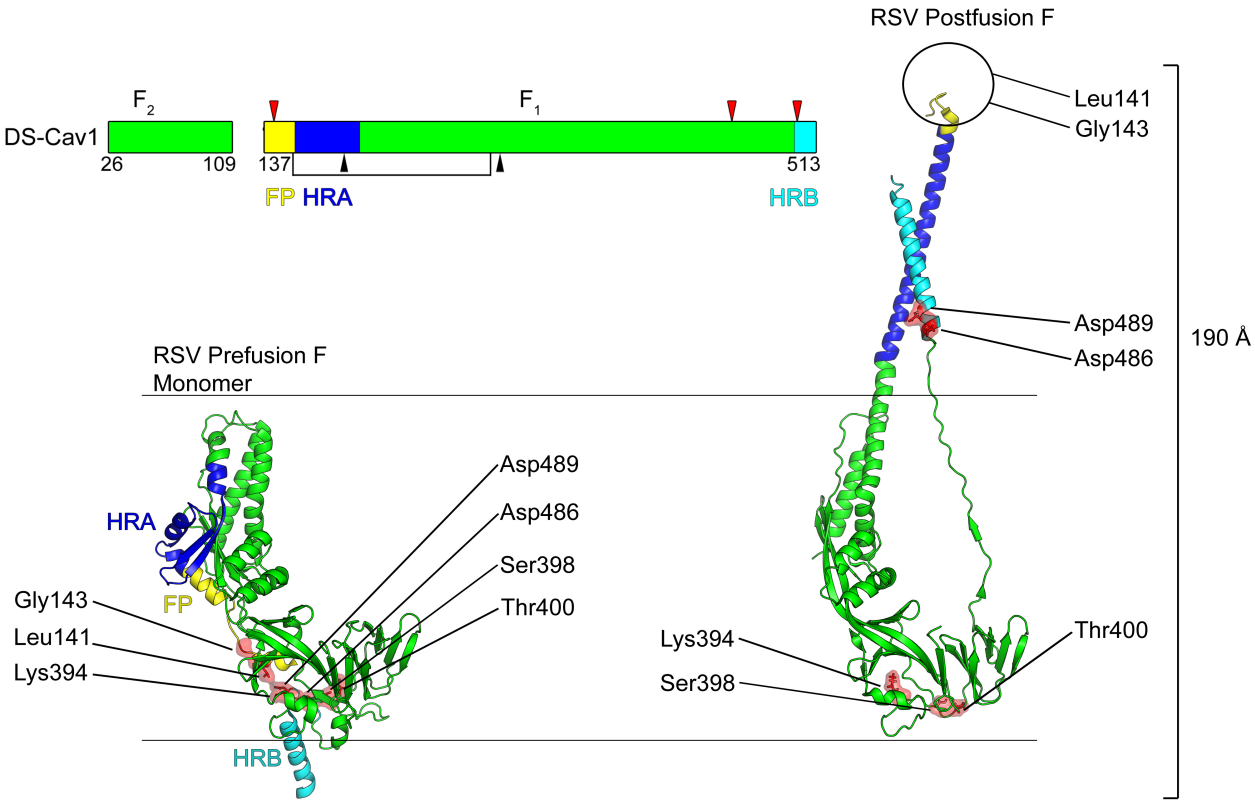

Supplementary Figure 1 | Inhibitor resistance mutations cluster near a cavity inside prefusion RSV F. Resistance mutations are clustered together in the prefusion structure, yet are distantly separated in the postfusion structure. Structures of an RSV F monomer in the prefusion (*left*) and postfusion (*right*) conformation are shown as ribbons. Residues commonly mutated in escape variants are shown as red transparent molecular surfaces. Fusion peptide (FP) is colored yellow, heptad repeat A (HRA) is shown in blue and heptad repeat B (HRB) is shown in cyan. The circled region denotes the first ten amino acids of the FP that are not present in the postfusion structure. Inset: Schematic of the mature RSV F protein in the DS-Cav1 construct. The prefusion-stabilizing disulfide bond and cavity filling mutations are shown as a black line and as black triangles, respectively. Clusters of escape mutations are depicted as red triangles.

Nature Chemical Biology: doi:10.1038/nchembio.1982

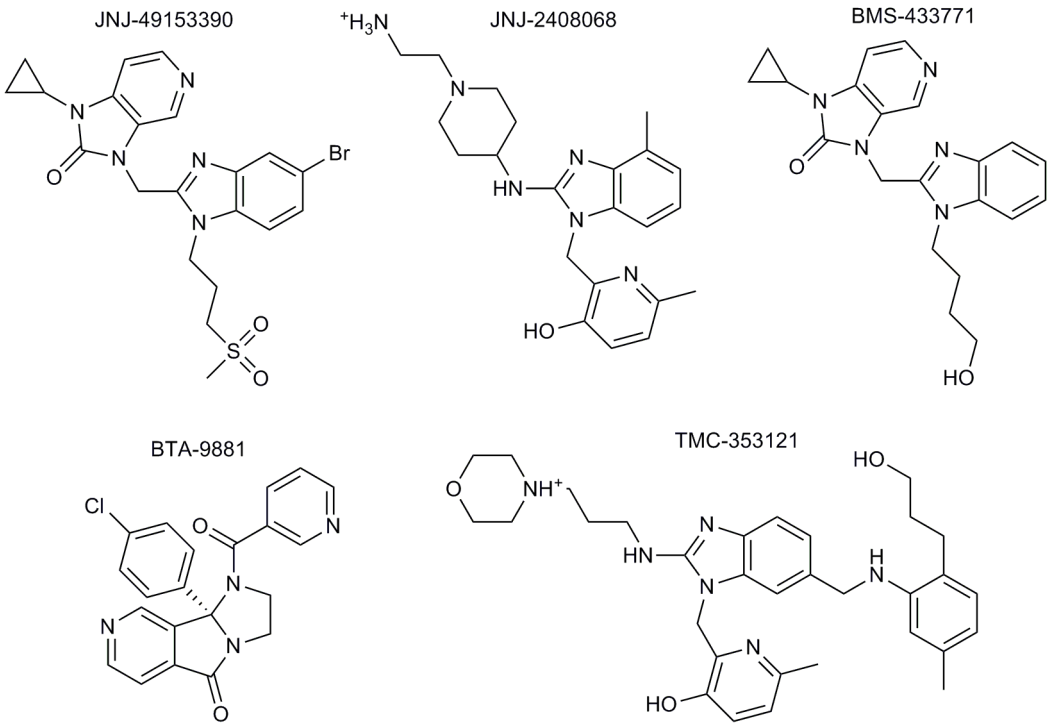

Supplementary Figure 2 | Chemical structures at physiological pH of fusion inhibitors used in this study.

Nature Chemical Biology: doi:10.1038/nchembio.1982

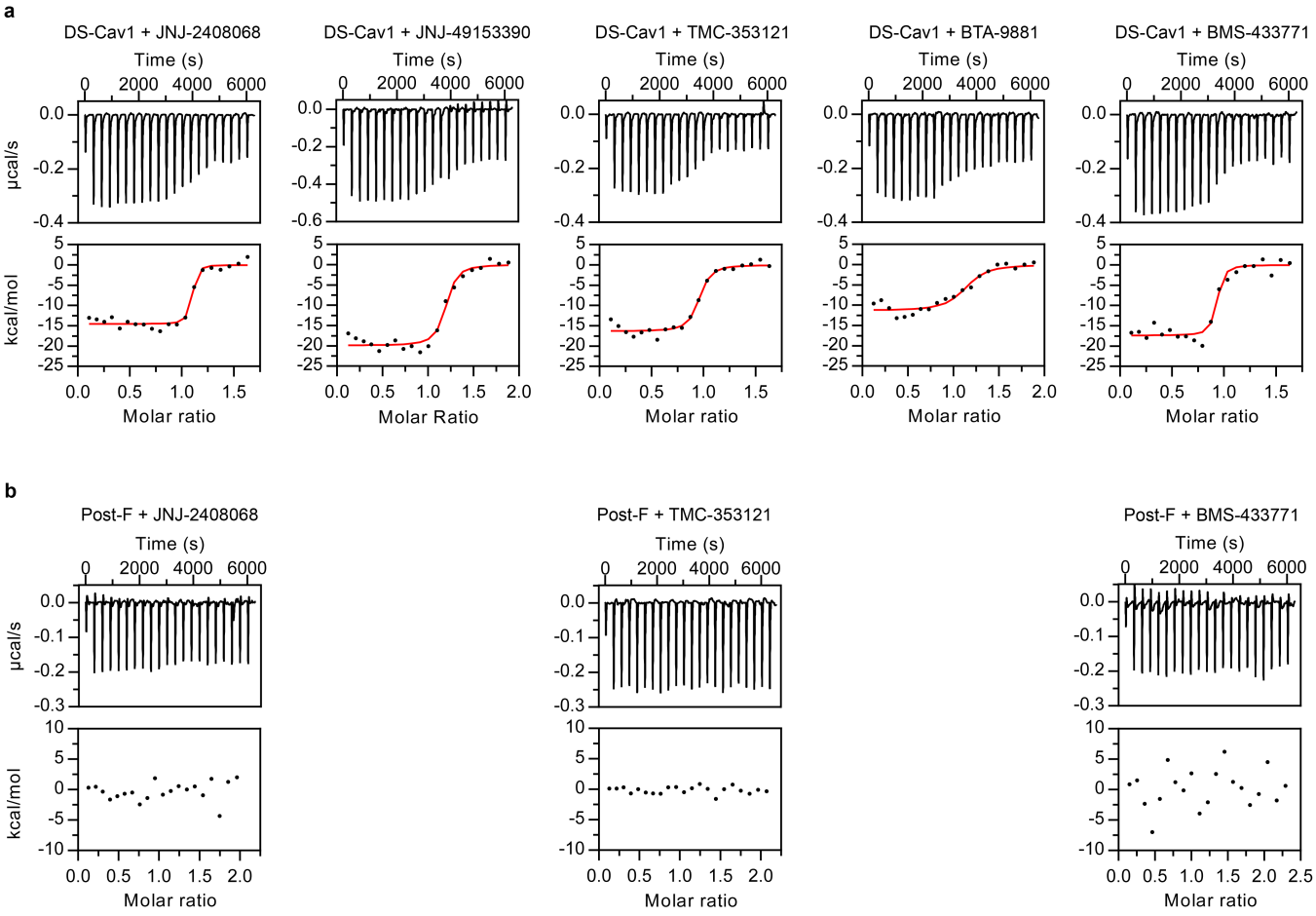

Supplementary Figure 3 | Inhibitors specifically bind to prefusion RSV F. ITC data for the binding of (**a**) five fusion inhibitors to prefusion RSV F (DS-Cav1) and (**b**) three of the compounds to postfusion RSV F. Data for JNJ-2408068 and JNJ-49153390 binding to DS-Cav1 are shown in the main text Figure 1a, but are also shown here to aid comparisons. Red lines represent the best fit of the data to a single-binding-site model.

Nature Chemical Biology: doi:10.1038/nchembio.1982

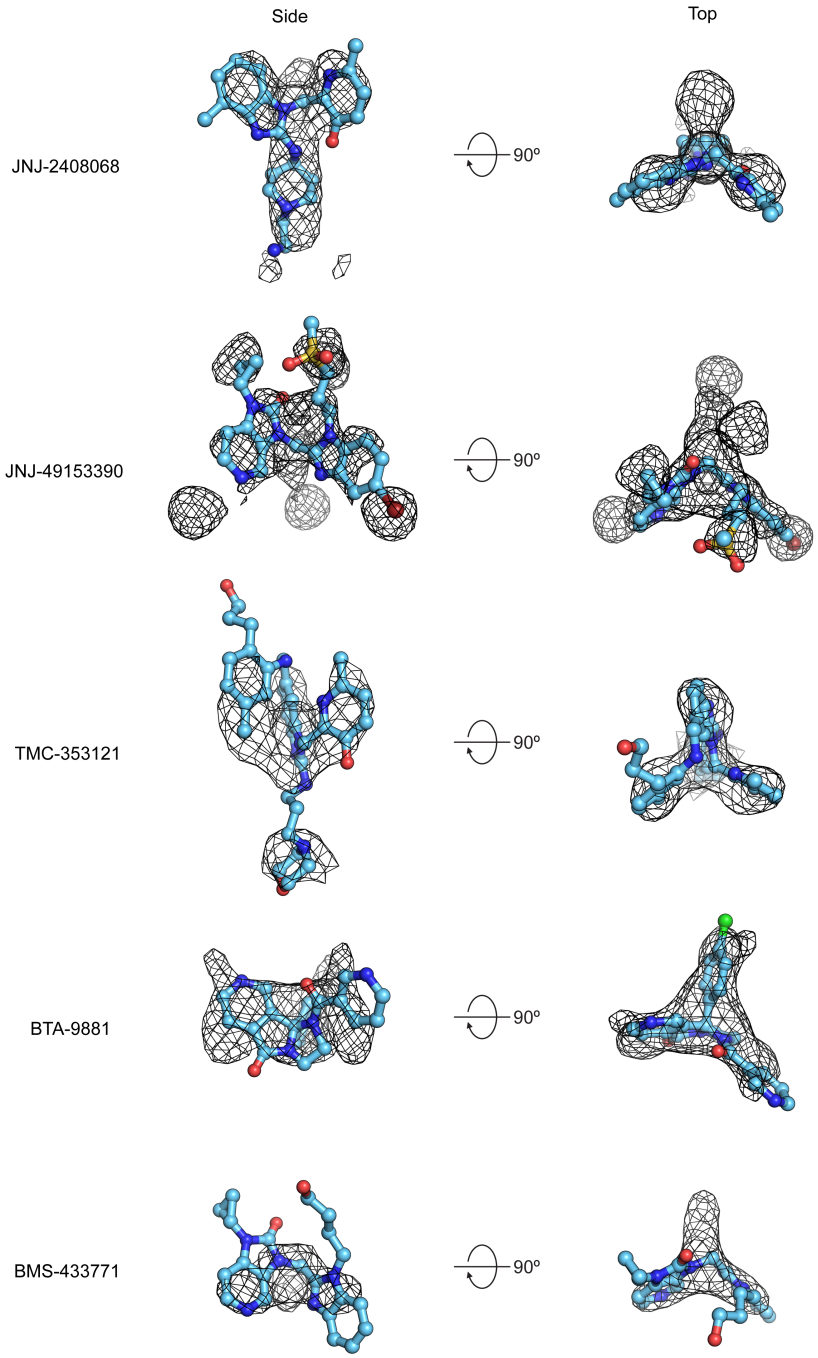

Supplementary Figure 4 | Electron density of inhibitors in the prefusion RSV F cavity exists as a 3-fold average. Inhibitors are shown in ball-and-stick representation with carbon atoms colored in cyan, nitrogen atoms in blue, oxygen atoms in red, bromine atoms in dark red, chlorine atoms in green, and sulfur atoms in yellow. Corresponding Fo-Fc electron density at 3.0 sigma is shown as a black mesh with a 2.1 Å carve. Fo-Fc density was calculated from SA omit maps generated in PHENIX after simulated-annealing refinement with the inhibitor occupancy set to 0.0 and with zero occupancy atoms ignored during refinement. Side and top views are related by a 90° rotation about the horizontal axis.

Nature Chemical Biology: doi:10.1038/nchembio.1982

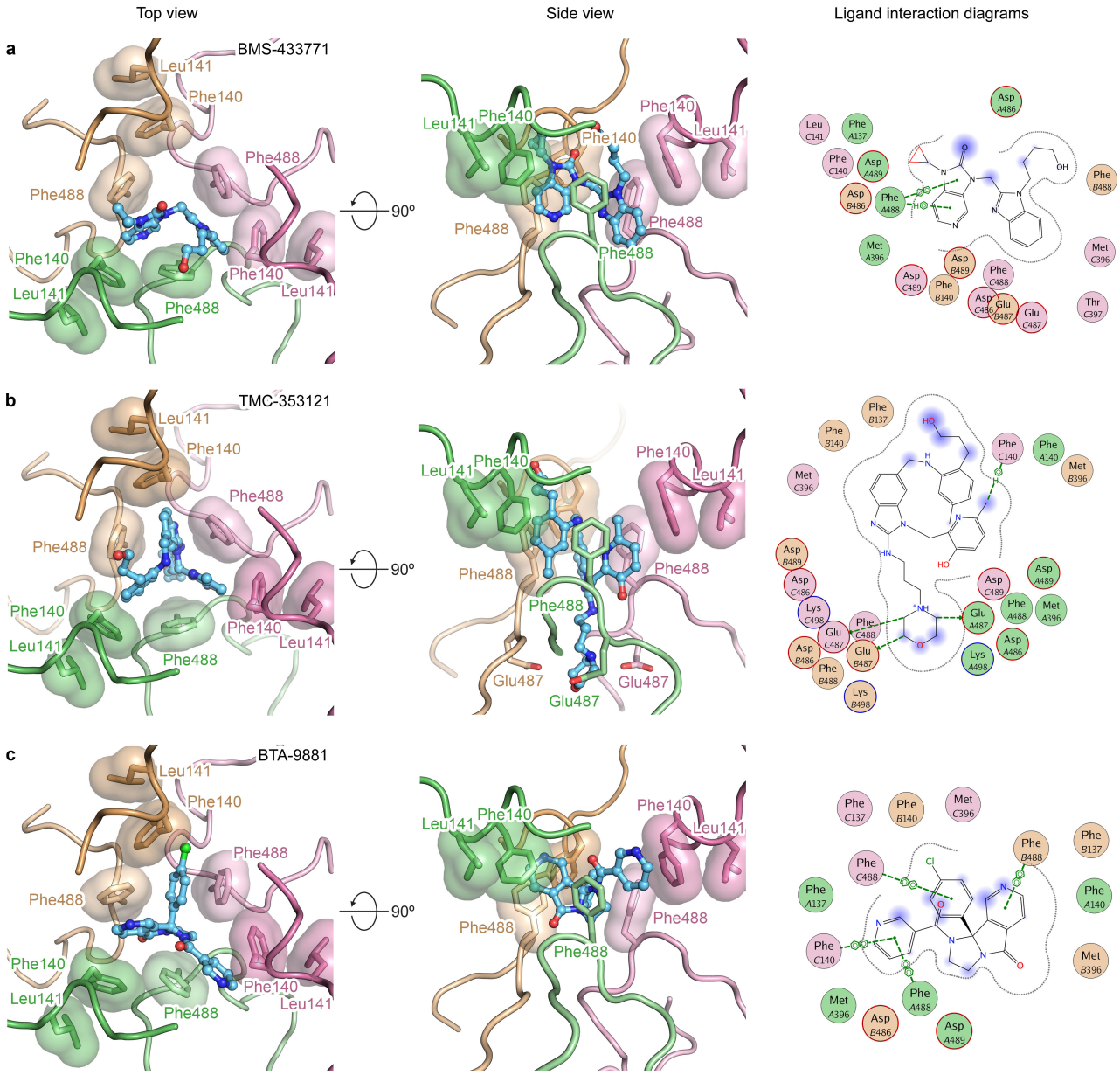

Supplementary Figure 5 | Inhibitors BMS-433771, TMC-353121, and BTA-9881 tether hydrophobic residues in two structurally labile regions. Top (*left*) and side (*middle*) views of the interactions between (**a**) BMS-433771, (**b**) TMC-353121 and (**c**) BTA-9881 with RSV F. Each RSV F protomer is a different color (tan, pink and green), and hydrophobic side-chains are shown with transparent molecular surfaces. Inhibitors are shown as ball-and-stick, with carbon atoms colored in cyan, nitrogen atoms in blue, oxygen atoms in red, and chlorine atoms in green. (*right*) 2D ligand-interaction diagrams generated in Molecular Operating Environment. Bonds with RSV F side-chain atoms are shown as green dashed lines, and when present arrowheads point toward the acceptor.

Nature Chemical Biology: doi:10.1038/nchembio.1982

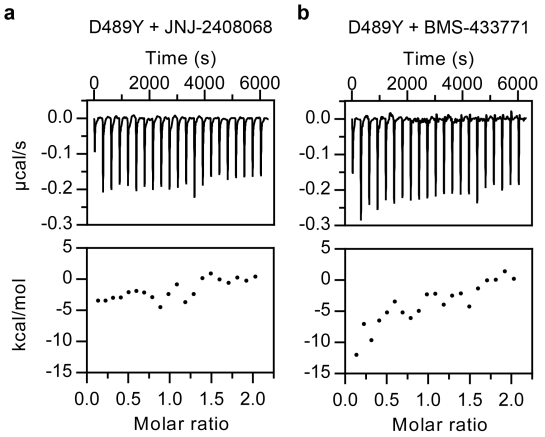

Supplementary Figure 6 | JNJ-2408068 and BMS-433771 bind poorly to resistance mutant D489Y. ITC data for the binding of (**a**) JNJ-2408068 and (**b**) BMS-433771 to the DS-Cav1 D489Y variant. Due to the substantially reduced affinity of the inhibitors for the D489Y variant, reliable fits of the data to a single-binding-site model could not be obtained.

Nature Chemical Biology: doi:10.1038/nchembio.1982

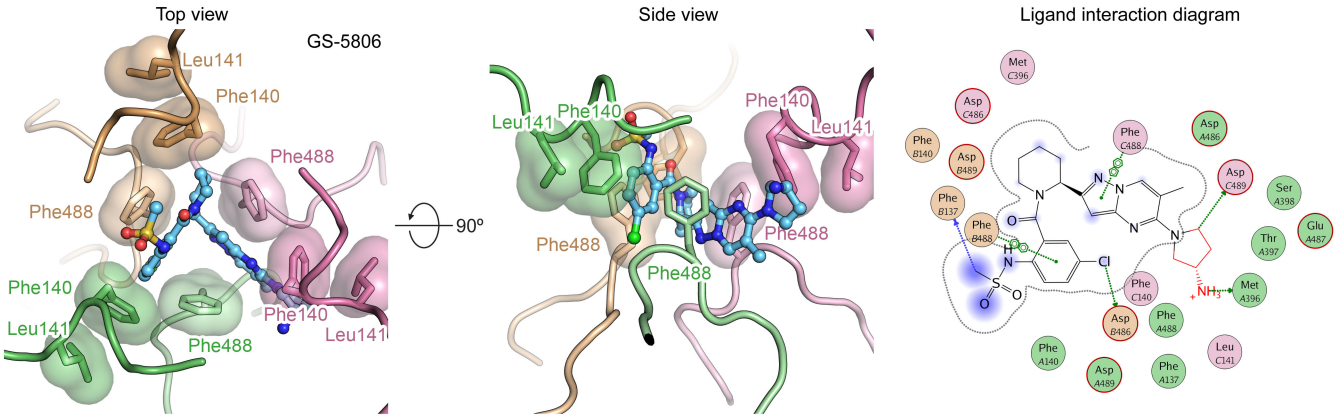

Supplementary Figure 7 | Model of GS-5806 bound to prefusion RSV F. Top (*left*) and side (*middle*) views of the possible interactions between GS-5806 and RSV F. Each RSV F protomer is a different color (tan, pink and green), and hydrophobic side-chains are shown with transparent molecular surfaces. Inhibitors are shown as ball-and-stick, with carbon atoms colored in cyan, nitrogen atoms in blue, oxygen atoms in red, chlorine atoms in green and sulfur atoms in yellow. (*right*) 2D ligand-interaction diagram generated in Molecular Operating Environment. Bonds with RSV F main-chain and side-chain atoms are shown as blue and green dotted lines, respectively, and when present the arrowhead points toward the acceptor. All panels are based on the docking of GS-5806 into the structure and electron density of JNJ-49155390 bound to RSV F. GS-5806 was overlapped onto JNJ-49155390 using the program ROCS (Rapid Overlay of Chemical Structures, ver 3.2.0.4)[1]. The ROCS run was carried out with the following parameters: "rankby = combo" and other parameters as default. The query was the co-crystal structure of JNJ-49155390, whereas the database of conformers was generated by OMEGA (ver 2.5.1.4)[2] for the GS-5806 reference compound. The combo score (the similarity score calculated) was in the range of 0.69-0.81 for the 100 best-ranked conformations. Conformation "15" of GS-5806 disclosed the best fit with the JNJ-49155390 electron density. Additional manipulation of GS-5806 was performed manually in *Coot*[3]. In this pose, there is a clash of the pyrrolidin-3-aminium group with Phe140, but this could be eliminated by minor movement of the protein.

Nature Chemical Biology: doi:10.1038/nchembio.1982

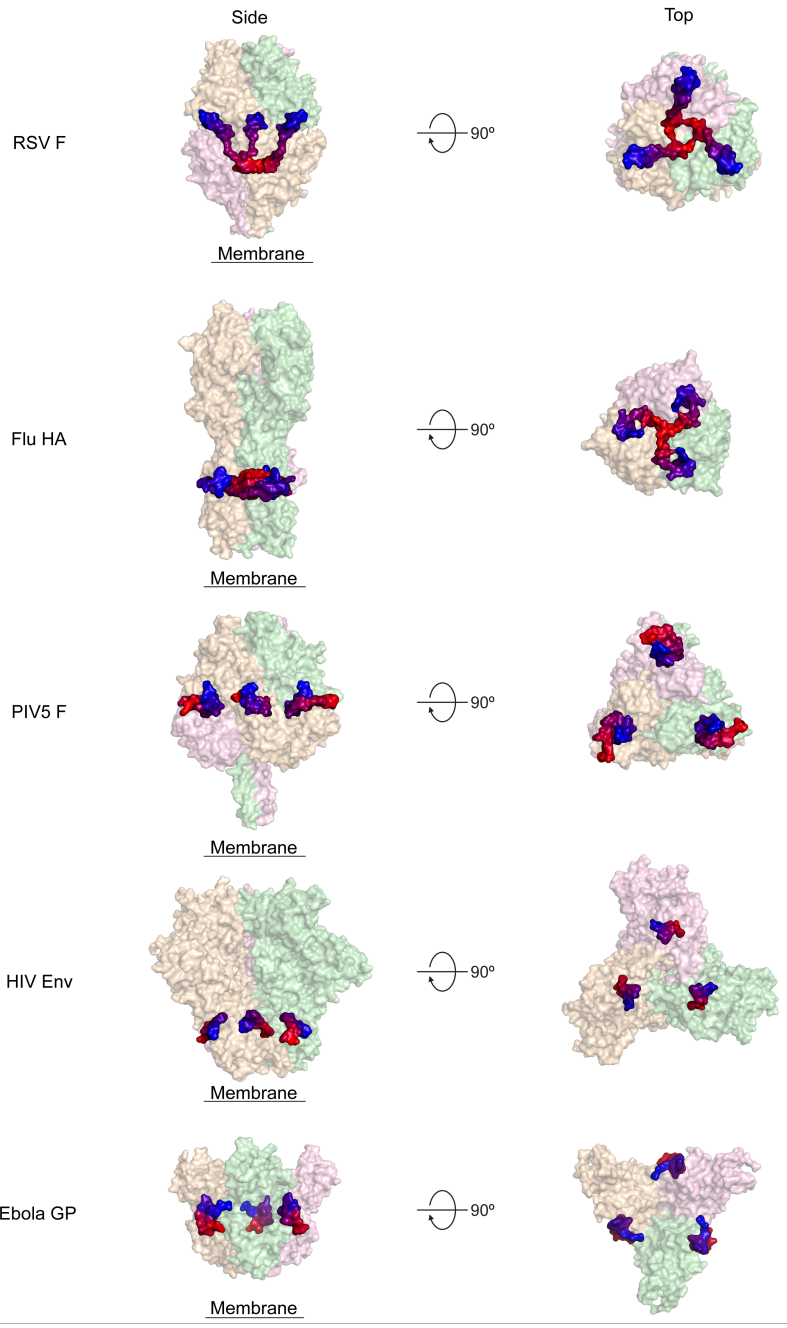

Supplementary Figure 8 | Fusion peptide locations in class I viral fusion glycoproteins. Prefusion structures of JNJ-2408068-bound RSV F, influenza HA [PDB ID: 2HMG[4]], PIV5 F [PDB ID: 4GIP[5]], HIV Env [PDB ID: 4TVP[6]] and Ebola GP [PDB ID: 3CSY[7]] are shown as transparent molecular surfaces. Each prefusion glycoprotein protomer is colored differently (tan, pink and green), and fusion peptides are shown as opaque molecular surfaces colored as a spectrum from red to blue, N-terminus to C-terminus, respectively. Side and top views are related by a 90° rotation about the horizontal axis. Note that instead of a canonical fusion peptide, Ebola GP has an internal fusion loop and thus lacks a free N-terminus. Thus, for GP the hydrophobic portion of the internal fusion loop is shown. For HIV Env, the first six amino acids (512–517) of the fusion peptide are not shown since these were disordered in the structure.

Nature Chemical Biology: doi:10.1038/nchembio.1982

Supplementary Table 1 Crystallographic data collection and refinement statistics

	JNJ-2408068	JNJ-49153390	TMC-353121	BTA-9881	BMS-433771	D489Y
Data collection						
Space group	$P4_132$	$P4_132$	$P4_132$	$P4_132$	$P4_132$	$P4_132$
Cell dimensions						
$a=b=c$ (Å)	170.1	168.4	169.9	170.2	169.6	168.2
α, β, γ (°)	90, 90, 90	90, 90, 90	90, 90, 90	90, 90, 90	90, 90, 90	90, 90, 90
Resolution (Å)	49.1–2.75 (2.90–2.75)*	48.6–2.30 (2.38–2.30)	49.0–3.05 (3.26–3.05)	49.1–2.75 (2.94–2.75)	41.1–2.85 (3.0–2.85)	48.6–2.60 (2.73–2.60)
R_{merge}	0.257 (3.73)	0.170 (1.76)	0.317 (2.379)	0.280 (3.695)	0.210 (1.669)	0.223 (2.870)
$I / \sigma I$	17.6 (1.9)	17.4 (1.8)	11.9 (1.6)	14.8 (1.5)	9.1 (2.0)	18.2 (1.6)
Completeness (%)	100.0 (100.0)	100.0 (100.0)	100.0 (100.0)	100.0 (100.0)	100.0 (100.0)	100.0 (100.0)
Redundancy	32.9 (20.2)	19.9 (16.1)	25.2 (23.5)	35.1 (31.4)	8.9 (9.2)	29.3 (28.4)
Refinement						
Resolution (Å)	49.1–2.75	48.6–2.30	49.0–3.05	49.1–2.75	41.1–2.85	48.6–2.60
Unique reflections	22,458 (2,746)	36,773 (2,782)	16,513 (2,657)	22,481 (2,741)	20,039 (2,802)	25,575 (2,795)
R_{work} / R_{free} (%)	19.9/22.9	17.9/21.4	21.4/24.8	20.4/23.5	19.6/24.1	19.9/23.7
No. atoms						
Protein	3,253	3,424	3,297	3,275	3,376	3,471
Inhibitor	29	31	41	28	28	-
Ligand/ion	43	38	28	33	38	48
Water	36	242	0	30	24	65
B-factors (Å^2)						
Protein	64.9	50.5	82.5	69.8	66.8	67.1
Inhibitor	36.9	36.8	64.4	77.8	60.8	-
Ligand/ion	121.9	95.7	102.8	121.4	134.3	113.3
Water	46.2	46.9	-	53.1	54.6	49.7
R.m.s. deviations						
Bond lengths (Å)	0.006	0.005	0.006	0.007	0.006	0.006
Bond angles (°)	0.89	0.89	0.88	0.98	0.98	0.93

Data were collected from one crystal for each structure
*Values in parentheses are for highest-resolution shell.

Nature Chemical Biology: doi:10.1038/nchembio.1982

Supplementary Table 2 Susceptibility of RSV strains harboring F variants

Virus strain	Mutation	JNJ-2408068		JNJ-49153390		TMC-353121		BMS-433771		BTA-9881	
		EC_{50}*	FC†	EC_{50}	FC	EC_{50}	FC	EC_{50}	FC	EC_{50}	FC
RSV224‖	WT	0.11	NA‡	0.16	NA	0.1	NA	6.8	NA	3,200	NA
	L141W	173	1,573	540	3,375	NM§	NM	>25,000	>3,676	>25,000	>8
	K394R/S398L	>5,000	>45,455	>1,000	>6,250	>1,000	>10,000	>25,000	>3,676	>25,000	>8
	S398L	>5,000	>45,455	>1,000	>6,250	>1,000	>10,000	>25,000	>3,676	>25,000	>8
	D486N	>5,000	>45,455	18	112	233	2,330	777	114	>25,000	>8
	D489Y	>4,863	>44,209	667	4,169	28	280	>25,000	>3,676	>25,000	>22
Long¶	WT	0.3	NA	0.1	NA	0.06	NA	2.9	NA	116	NA
	G143S	>5,000	>16,667	>1,000	>10,000	320	5,333	>25,000	>8,621	>25,000	>216
	T400A	>5,000	>16,667	>1,000	>10,000	36	600	>25,000	>8,621	>25,000	>216

* EC_{50} values are expressed in nM; † FC = fold change over WT; ‡ NA = not applicable; § NM = not measured
‖ Antiviral activity of compounds against the rgRSV224 strain determined using inhibition of GFP expression.
¶ Antiviral activity of compounds against the Long strain determined by quantifying RSV F RNA by qRT-PCR

Nature Chemical Biology: doi:10.1038/nchembio.1982

Supplementary Movie 1 | Conformational rearrangements in RSV F required for inhibitor binding.
A morph from the unbound to the JNJ-2408068-bound conformation as viewed looking down the RSV F 3-fold axis toward the viral membrane. Main-chain residues are depicted as ribbons with select side-chains shown as sticks. The three RSV F protomers are colored tan, pink and green. Oxygen atoms are colored red and nitrogen atoms are blue. Hydrogen bonds are depicted as black dotted lines. Fo-Fc electron density at 3.0 sigma from a simulated-annealing omit map is shown as a black mesh. The movie and the morph were generated in PyMOL v1.7 (Schrödinger, LLC).

Nature Chemical Biology: doi:10.1038/nchembio.1982

Supplementary References

1. Grant, J.A., Gallardo, M.A. & Pickup, B.T. A fast method of molecular shape comparison: A simple application of a Gaussian description of molecular shape. *J. Comput. Chem.* **17**, 1653-1666 (1996).

2. Bostrom, J., Greenwood, J.R. & Gottfries, J. Assessing the performance of OMEGA with respect to retrieving bioactive conformations. *J. Mol. Graph. Model.* **21**, 449-62 (2003).

3. Emsley, P., Lohkamp, B., Scott, W.G. & Cowtan, K. Features and development of Coot. *Acta Crystallogr. D Biol. Crystallogr.* **66**, 486-501 (2010).

4. Wilson, I.A., Skehel, J.J. & Wiley, D.C. Structure of the haemagglutinin membrane glycoprotein of influenza virus at 3 A resolution. *Nature* **289**, 366-73 (1981).

5. Welch, B.D. et al. Structure of the cleavage-activated prefusion form of the parainfluenza virus 5 fusion protein. *Proc. Natl. Acad. Sci. USA* **109**, 16672-7 (2012).

6. Pancera, M. et al. Structure and immune recognition of trimeric pre-fusion HIV-1 Env. *Nature* **514**, 455-61 (2014).

7. Lee, J.E. et al. Structure of the Ebola virus glycoprotein bound to an antibody from a human survivor. *Nature* **454**, 177-82 (2008).

Nature Chemical Biology: doi:10.1038/nchembio.1982